1-1-2016

X-ray Structure and Properties of the Ferrous Octaethylporphyrin Nitroxyl Complex

Nagabhushanam Kundakarla
Marquette University

Sergey V. Lindeman
Marquette University, sergey.lindeman@marquette.edu

Hafiz Md. Rahman
Marquette University

Michael D. Ryan
Marquette University, michael.ryan@marquette.edu

Accepted version. *Inorganic Chemistry*, Vol. 55, No. 5 (2016): 2070-2075. DOI.

X-ray Structure and Properties of the Ferrous Octaethylporphyrin Nitroxyl Complex

Nagabhushanam Kundakarla
Department of Chemistry, Marquette University
Milwaukee, WI
Sergey Lindeman
Department of Chemistry, Marquette University
Milwaukee, WI
Md. Hafiz Rahman
Department of Chemistry, Marquette University
Milwaukee, WI
Michael D. Ryan
Department of Chemistry, Marquette University
Milwaukee, WI

Synopsis: The X-ray crystal structure of $[Fe(OEP)(NO)]^{-}$ is reported, along with infrared and NMR spectra. The Fe−N−O bond angle decreased upon reduction and was consistent with those in other $\{FeNO\}^{8}$ complexes. The ^{1}H NMR spectrum was reported, which was different from those for other $S = 0$ metalloporphyrin complexes due to the displacement of the Fe atom from the porphyrin plane. This spectrum was consistent with DFT calculations.

Inorganic Chemistry, Vol 55, No. 5 (2016): pg. 2070-2075. DOI.

Abstract

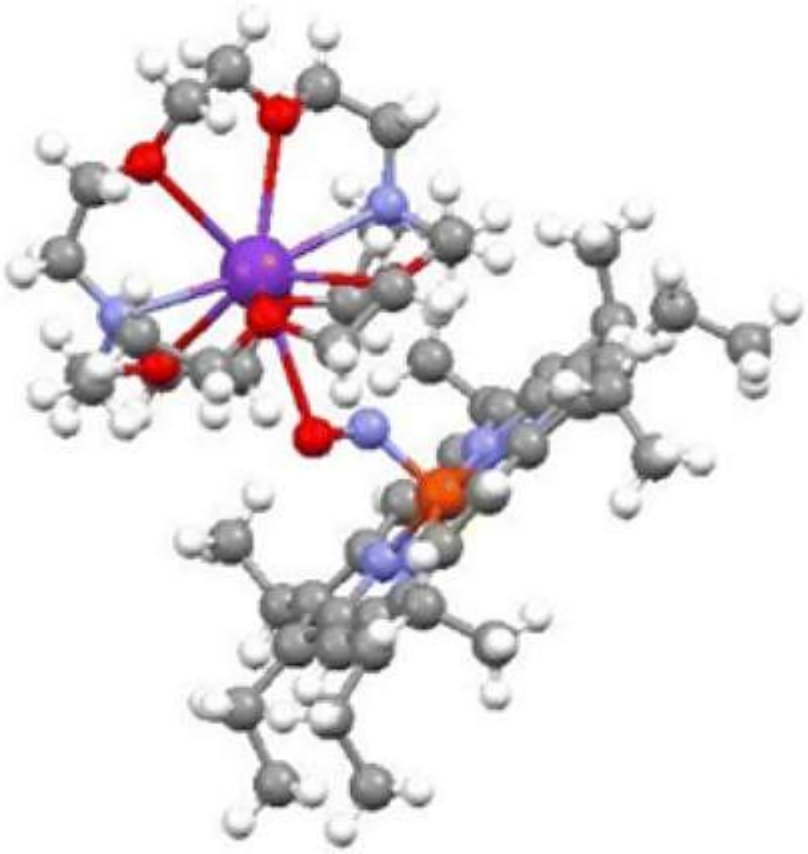

The preparation and characterization of the iron octaethylporphyrin nitroxyl ion, [Fe(OEP)(NO)$^{-}$], is reported. The complex was synthesized by the one-electron reduction of Fe(OEP)(NO) using anthracenide as the reducing agent. The compound was isolated as the potassium (2.2.2)cryptand salt. The anion was characterized using X-ray analysis with visible and infrared spectroscopy. The spectral features of the iron nitroxyl complex were consistent with previous literature reports. The important structural changes upon reduction were a significant decrease in the Fe–N–O bond angle from 142° to 127° and an increase in the N–O bond length from that in the starting nitrosyl moiety. The porphyrin ring became significantly less planar upon reduction, but the displacement of the iron atom from the 24-atom plane was essentially unchanged. In spite of the attempt to encapsulate the potassium ion with the (2.2.2)cryptand, significant interaction between K^{+} and the oxygen of the nitroxyl were observed, indicating a contact ion pair in the crystal structure. Comparison between the experimental structure and the DFT-calculated parameters were reported. The results are consistent with the Fe–N–O moiety being the site of the reduction, with little evidence for the reduction of the iron itself or the porphyrin ring. The proton NMR spectrum was also obtained,

Inorganic Chemistry, Vol 55, No. 5 (2016): pg. 2070-2075. DOI.

and the chemical shifts were significantly different from other $S = 0$ metalloporphyrin complexes. These shifts, though, were consistent with the DFT calculations.

Introduction

Iron porphyrin nitroxyl compounds have attracted considerable interest due to their varied chemical and biochemical reactions. The nitroxyl, along with its conjugate acid (HNO), is involved in a number of biochemical processes, including microbial denitrifying enzymes,[1] as well as providing therapeutic benefits.[2,3] Ferrous nitroxyl species have been proposed as intermediates in nitric oxide reductase (NorBC)[4] and cytochrome P450nor.[5,6] The electronic structure and biological reactivity of Fe(HNO) complexes have been recently reviewed.[7] Particular interest has been focused on $[Fe(P)(NO)]^-$ because of its relationship to Fe(P)(HNO) (where P = porphyrin). The cyclic voltammetry of Fe(OEP)(NO) and Fe(TPP)(NO) (OEP = octaethylporphyrin; TPP = tetraphenylporphyrin) was reported by Olson et al.[8,9] In the latter work, the visible spectroelectrochemistry of the oxidation and reduction of these complexes was reported.[9] Choi and Ryan[10] examined the voltammetry of Fe(TPP)(NO) in the presence of amines. Mu and Kadish[11] used FTIR spectroelectrochemistry to characterize the ν_{NO} band in $[Fe(P)(NO)]^+$. Choi et al.[12] used resonance Raman spectroscopy to obtain the spectrum of $[Fe(TPP)(NO)]^-$ in THF, and identify its ν_{NO} and $\nu_{Fe\text{-}NO}$ bands. The FTIR spectroelectrochemistry of Fe(OEP)(NO) was reported by Wei and Ryan,[13] and measured the ν_{NO} band of $[Fe(OEP)(NO)]^-$ to be 1441 cm^{-1}, a decrease of 229 cm^{-1} upon reduction. Goodrich et al.[14] used visible and FTIR spectroelectrochemistry to study the reduction of a bis picket fence porphyrin nitrosyl and observed a similar decrease in the ν_{NO} band in the infrared.

Scheidt and Frisse[15] reported on the X-ray structure of Fe(TPP)(NO). Two crystal structures of Fe(OEP)(NO) were later reported by Scheidt et al.[16] Prior to this work, iron porphyrin nitrosyl structures suffered from disorder.[15,17,18] Later Goodrich et al.[14] also obtained a single NO orientation with a bis picket fence iron porphyrin. All of the structures showed a bent Fe–N–O moiety, with an angle of about 144° and a tilt of about 6–8°. The structures of two ferric porphyrin nitrosyl complexes, $[Fe(TPP)(NO)][ClO_4]$ and

Inorganic Chemistry, Vol 55, No. 5 (2016): pg. 2070-2075. DOI.

[Fe(TPP)(NO)(H_2O)][ClO_4], were reported by Scheidt et al.[19] The Fe–N–O bond angles were about 175–177°, close to linear. The isolation of the first {FeNO}^{8} porphyrin complex, [Fe(TFPPBr_8)(NO)]$^-$ (TFPPBr_8 = tetrakis(pentafluorophenyl)octabromoporphyrin), was reported by Pellegrino et al.[20] The ν_{NO} value for the complex decreased from 1715 to 1547 cm^{-1}, consistent with previous solution studies of Fe(P)(NO)$^-$.[12-14] Recently, the structure of [Fe(TFPPBr_8)(NO)]$^-$ was reported.[21] An Fe–N–O bond angle of 122° was reported for this complex. The isolation of [Fe(OEP)(NO)]$^-$ has not yet been reported. The octaalkylporphyrins are structurally much closer to the physiological porphyrins than is TFPPBr_8, and the isolation and characterization of this complex would be of great value. In this paper, we report on the X-ray crystal structure of [Fe(OEP)(NO)]$^-$.

Experimental Section

Iron octaethylporphyrin chloride, zinc octaethylporphyrin, THF, 2.2.2-cryptand (4,7,13,16,21,24-hexaoxa-1,10-diazabicyclo[8.8.8]hexacosane), anthracene, and THF were obtained from Sigma-Aldrich Chemical Co. The nitrosyl complex Fe(OEP)(NO) (**1**) and its ^{15}N analogue were synthesized by literature methods.[22] Meso-deuteration of H_2OEP was accomplished using the D_2SO_4/D_2O method.[23] 1-Methylimidazole-d_3 was obtained from CDN Isotopes. Anhydrous tetrahydrofuran (THF) was refluxed in the presence of sodium and benzophenone under nitrogen until the solution was blue. The reducing agent, a 0.20 M solution of the potassium cryptand salt of anthracenide, was generated in the glovebox by dissolving equimolar amounts of anthracene and 2.2.2-cryptand in THF. A small amount of potassium metal was then added to this solution. After reaction, the excess potassium metal was removed and disposed of properly. Caution: potassium metal is very reactive and can cause fire or explosion due to the formation of H_2 and the exothermicity of its reaction with water or acidic protons. The complex Fe(OEP)(NO) was dissolved in THF, and 1 equiv of potassium cryptand anthracenide was added. The solvent was removed, and the solid was then redissolved in THF. Crystallization was obtained by layering with heptane. The infrared spectra were obtained with a Thermo Nicolet-FTIR spectrophotometer (Model 670 Nexus) with an MCT detector. Infrared spectra of solid materials were collected as KBr pellets. Analysis of the

Inorganic Chemistry, Vol 55, No. 5 (2016): pg. 2070-2075. DOI.

crystal packing distances and planarity of the porphyrin ring was carried out using the program MERCURY from the Cambridge Crystallographic Data Center (University of Cambridge, Cambridge, U.K.). ^{1}H NMR spectra were collected at room temperature with a Varian 400 MHz spectrometer.

Electronic structure, NMR, and vibrational spectral calculations were carried out using the m06, m06L, mpwvwn, and bp86 DFT functionals and the TZVP basis set for all elements except for the iron atom using the Gaussian 09 suite of programs.[24-26] Only the m06 functional was used for the NMR calculations. The Wachters basis set was used for iron.[27] All calculations converged using the tight optimization criteria.

Results and Discussion

X-ray Crystal Structure

The reduction of Fe(OEP)(NO) (**1**) was carried out using potassium (2.2.2)cryptand anthracenide as the reducing agent as described in the Experimental Section. The visible spectrum of the chemically generated $[Fe(OEP)(NO)]^{-}$ was consistent with the literature values.[9,12,28] The ferrous nitroxyl complex $[Fe(OEP)(NO)]^{-}$ (**2**) was crystallized as the potassium cryptand salt. The salt crystallized with two cations, two anions, and one anthracene molecule in an asymmetric unit. In general, the bond lengths and angles of both porphyrin structures in the asymmetric unit were within experimental error. There are two important exceptions: the K1–O1 (K1A–O1A; 3.125 and 3.278 Å, respectively) and O1–N5 (O1A–N5A) (Table 2) distances differed by more than the experimental error. While the K1–O1/K1A–O1A distances differed, the K1–O1–N5/K1A–O1A–N5A bond angles were similar (98.57° versus 98.36°, respectively), but the uncertainties were large (0.18°). These differences in the ionic bond lengths (K–O distance) and the uncertainties in the K–O–N bond angles are probably due to the thermal motion of the NO group. The stronger the thermal motion, the shorter the bond will appear.[32] In our case, the thermal vibrations of the O and N atoms forming the shorter N═O bond are 20–25% stronger than the longer bond. The structure of the cation and anion is shown in Figure 1, and the crystallographic

Inorganic Chemistry, Vol 55, No. 5 (2016): pg. 2070-2075. DOI.

data and structure refinement details are shown in Table 1. Additional structural data are given in the Supporting Information. The important bond lengths and angles are shown in Table 2, along with a comparison with those of related complexes.

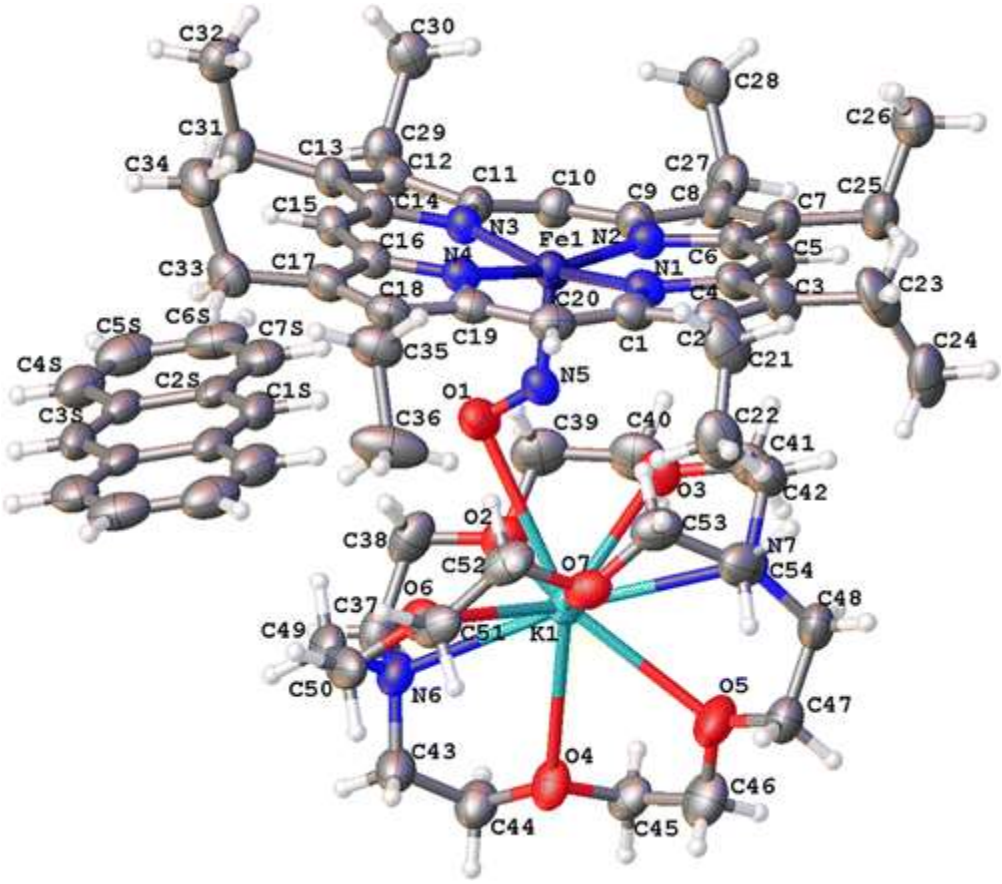

Figure 1. ORTEP diagram for one of the [K(2.2.2)][Fe(OEP)(NO)] units in the asymmetric unit. Ellipsoids are depicted at 50% probability.

Table 1. Crystal Data and Structure Refinement Details for [K(2.2.2)-cryptand][Fe(OEP)(NO)]·0.5(anthracene)

empirical formula	$C_{61}H_{85}FeKN_7O_7$
formula wt	1123.31
temp/K	100.00(10)
cryst syst	triclinic
space group	$P\bar{1}$
a, Å	14.7775(2)
b, Å	19.6688(3)
c, Å	21.2458(3)
α, deg	83.4024(14)
β, deg	88.8922(12)

γ, deg	73.4501(14)
V, Å^3	5879.61(16)
Z	4
ρ_{calcd}, g/cm^3	1.269
μ, mm^{-1}	3.148
F(000)	2404.0
cryst size, mm^3	0.633 × 0.139 × 0.113
radiation	Cu Kα (λ = 1.54184)
2θ range for data collection, deg	5.94–148.4
index ranges	$-18 \le h \le 18$, $-23 \le k \le 24$, $-26 \le l \le 26$
no. of rflns collected	111300
no. of indep rflns	23568 (R_{int} = 0.0502, R_σ = 0.0373)
no. of data/restraints/params	23568/45/1392
goodness of fit on F^2	1.021
final R indexes ($I \ge 2\sigma(I)$)	R1 = 0.0625, wR2 = 0.1502
final R indexes (all data)	R1 = 0.0797, wR2 = 0.1610
largest diff peak/hole, e Å^{-3}	1.12/-0.63

Table 2. Selected Crystallographic Determined Parameters and Nitrosyl Infrared Energies for Related Metalloporphyrin Nitrosyl Complexes

complex		$M–N_{NO}$, Å	N–O, Å	$(M–N_p)_{av}$, Å	M–N–O, deg	ν_{NO}, cm^{-1}	$E°$, V vs SCE	ref
Fe(OEP)(NO)	SC	1.7307(7)	1.168(1)	2.009(12)	142.74(8)	1673	–1.10	[8, 16]
[Fe(OEP)(NO)]$^-$	SC	1.812(3), 1.816(3)	1.187(3), 1.203(3)	1.993(16), 1.993(16)	127.2(2), 126.8(2)	1445 (1428)[a]		[13], this work
	DFT/m06	1.786	1.190	2.002	122	1530		this work
	DFT/m06L	1.787	1.197	2.008	123	1503		this work
	DFT/bp86	1.783	1.207	2.012	125	1527		this work
	DFT/mpwvwn	1.809	1.213	2.041	125	1480		this work
Fe(TFPPBr$_8$)(NO)	SC	1.741(5)	1.131(6)	1.988(12)	148.5(4)	1718	–0.16	[20, 21]
[Fe(TFPPBr$_8$)(NO)]$^-$	SC	1.814(4)	1.194(5)	1.972(11)	122.4(3)	1540		[21]
[Fe(porphine)(NO)]$^-$	DFT	1.798	1.211		123	1530		[20]
	DFT	1.786	1.206	2.011	125	1533		[14]
Co(OEP)(NO)	SC	1.8444(9)	1.164(1)	1.984(8)	123.4(2)	1677	–1.15[b]	[29, 30]
	SC	1.844(2)	1.152(3)	1.985(9)	123.39(5)	1675		[31]

[a] [Fe(OEP)(^{15}NO)]$^-$ [b] Fe(TPP)(NO).

As was observed for [Fe(TFPPBr$_8$)(NO)]$^-$ (**3**),[21] the Fe–N–O bond angle decreased significantly when the nitrosyl complex was reduced.

Inorganic Chemistry, Vol 55, No. 5 (2016): pg. 2070-2075. DOI.

For **2**, the bond angle (average) decreased from 144 to 127°, a decrease of 17° (Fe–N–O angles for each anion 126.8(2) and 127.2(2)°). This compares to a slightly smaller bond angle of 122.4° for **3**. The Fe–N–O bond angle of **3** and the Co–N–O bond angle of Co(OEP)(NO) were similar (**3**, 122.4°; Co(OEP)(NO), 122.7 and 123.4°); all three structures had bond angles smaller than the angle in $[Fe(OEP)(NO)]^-$. The Fe–N–O angle was consistent with the formation of a $\{FeNO\}^8$ structure. Upon reduction, the tilt angle for Fe–N decreased from 6° to 8° in **1** and to 2° in **2**. The N–O bond length (average) in **2** was 1.195 Å, which was essentially the same as the bond length in **3** (1.194 Å).

The distances between the potassium ion and the nearest atom of the axial ligand are within the range observed for other metalloporphyrins. For example, comparing salts with a K(2.2.2) cation, a shorter K–N distance of 2.957 Å was observed for $K^+(2.2.2)[Fe(TPP)(CN)_2]^{2-}$,[33] while a longer K–O distance was seen in $[Co^{III}(TPP)(NCO)_2]^-$ (3.407 Å).[34] The interaction of the cation with the $Fe(P)(NO)^-$ anion is significantly different in our work as compared to that of Hu and Li.[21] In Hu and Li's work, the N–O moiety was directed away from the cation, $[Co(Cp)_2]^+$, which showed no specific interaction with the anion. In our work, the distances were relatively short (around 3.2 Å) between K1 and O1, similar to the potassium cryptand salt of $[Fe^{II}(TPP)(CN)_2]^-$, where there was a similar interaction between the K(2.2.2) ion and the N atom of the cyanide ligands. This is consistent with a contact ion pair, on the basis of the work of Davlieva et al.[35]

The average Fe–N_p bond distance decreased upon reduction from 2.009 Å (2.004 Å for structure B) to 1.993 Å (0.016/0.011 Å), where N_p is the average distance between the iron atom and the four pyrrole nitrogens of OEP. This decrease was similar to that observed for $[Fe(TFPPBr_8)(NO)]^-$, where the average distance decreased from 1.988 to 1.972 Å (0.016 Å). For Fe(OEP)(NO), the displacements of Fe from the 24-atom porphyrin ring[16] were 0.29 and 0.27 Å for the two structures, while the Fe displacement for $[Fe(OEP)(NO)]^-$ was found to be 0.28 Å. This contrasts with $Fe(TFPPBr_8)(NO)$, where the Fe displacement decreased from 0.36 to 0.19 Å upon reduction.

Inorganic Chemistry, Vol 55, No. 5 (2016): pg. 2070-2075. DOI.

A small degree of ruffling was observed for the starting complex, Fe(OEP)(NO). The average deviation from the 24-atom plane was found to be 0.031 and 0.044 Å for the two structures that have been characterized.[16] Upon reduction, there was a significant increase in the nonplanarity of the porphyrin ring. This can be visually seen by the green structure in Figure 2. The average deviation of each atom in **2** from the 24-atom plane was 0.12 Å, 2–3 times larger than in Fe(OEP)(NO) (see Figure 2B for the individual displacements of $[Fe(OEP)(NO)]^-$; there were no significant differences between the two anions in the unit cell). A comparison of Fe(OEP)(NO) (structure A) with **2** is shown in Figure 2, where **2** is the green structure and **1** is the pink structure. As can be seen, the nitroxyl is more saddled than the starting nitrosyl. The ruffling and saddling in **3** was significantly larger than in **2** (0.49 Å versus 0.12 Å), but the starting complex for **3** was already significantly saddled (0.51 Å).[21] Therefore, it would be difficult to detect and interpret changes that occurred upon the formation of **3**.

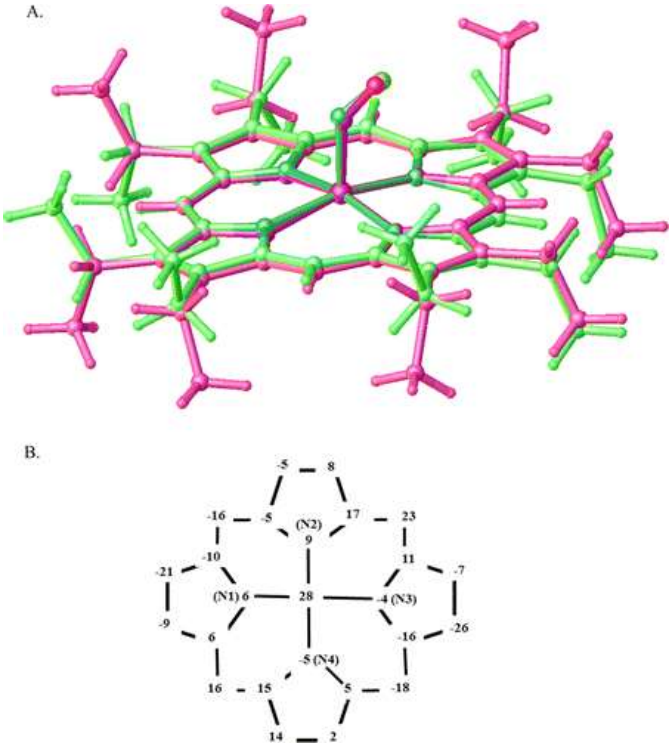

Figure 2. (A) Comparison of $[Fe(OEP)(NO)]^-$ (green) with Fe(OEP)(NO)[16] (structure A in the reference, pink). Hydrogens have been omitted for clarity. (B) Porphyrin core diagram that indicates the out-of-plane displacements of the atoms from the 24-atom porphyrin plane of $[Fe(OEP)(NO)]^-$ (first structure in unit cell, F1–C54). Displacements are given in units of 0.01 Å. Positive displacements are toward the nitroxyl group. Nitrogen atoms are labeled for orienting the ion. The nitroxyl is between N3 and N4.

For comparison, DFT was used to calculate the structure and infrared spectrum of $[Fe(OEP)(NO)]^-$, using the m06, m06L, mpwvwn, and bp86 functionals. The results are shown in Table 2. The infrared spectra of $[Fe(OEP)(NO)]^-$ (natural abundance) and $[Fe(OEP)(^{15}NO)]^-$ are shown in Figure 3. The ν_{NO} values observed for the solid nitroxyl complexes are consistent with those previously reported by spectroelectrochemistry.[13] For many parameters, there was good agreement between the calculated and experimental values. The two distances for the length of the N–O bond in the two anions within the asymmetric unit were within the range predicted by the DFT calculations (DFT, 1.190 and 1.213 Å; experimental, 1.187 and 1.203 Å). The Fe–NO distances by DFT were shorter than the experimental value, while the experimental Fe–N–O angle (127°) was only slightly larger than the DFT values (122–125°). On the one hand, the $Fe–N_p$ value was shorter (1.993 Å) than the predicted values (2.002–2.012 Å). On the other hand, the presence of two short and two long Fe–N bond distances was observed in both the experimental and DFT structures, in common with the Fe(OEP)(NO) starting complex. The DFT calculations all predicted shorter $Fe–N_{NO}$ distances (1.783–1.787 Å) than were observed in the crystal structure (1.812 Å). This indicates a weaker $Fe–N_{NO}$ bond than was predicted by the calculations. The lengthening of the N–O bond was consistent with the occupation of the π* orbital in N–O. This can be seen in the HOMO of $[Fe(OEP)(NO)]^-$ (Figure 4A), which was obtained from the m06/DFT calculations. NBO calculations of **1** and **2** show no significant change in the d orbital occupation of the iron atom, indicating little to no reduction of the iron itself. While there was considerable consistency in the DFT calculated structures between the functionals, there were differences in the electron distribution. The best correlation between the d orbital occupation and the IR frequency was for the sum of the $d_{x^2-y^2}/d_{z^2}$ orbitals. The sum was smallest for m06 (2.010, ν_{NO} 1530 cm^{-1}). As the sum of the $d_{x^2-y^2}/d_{z^2}$ orbitals increased, the calculated ν_{NO} frequency decreased (bp86, 2.090, ν_{NO} 1527 cm^{-1}; m06L, 2.195, ν_{NO} 1503 cm^{-1}; mpwvwn, 2.293, ν_{NO} 1480 cm^{-1})

Inorganic Chemistry, Vol 55, No. 5 (2016): pg. 2070-2075. DOI.

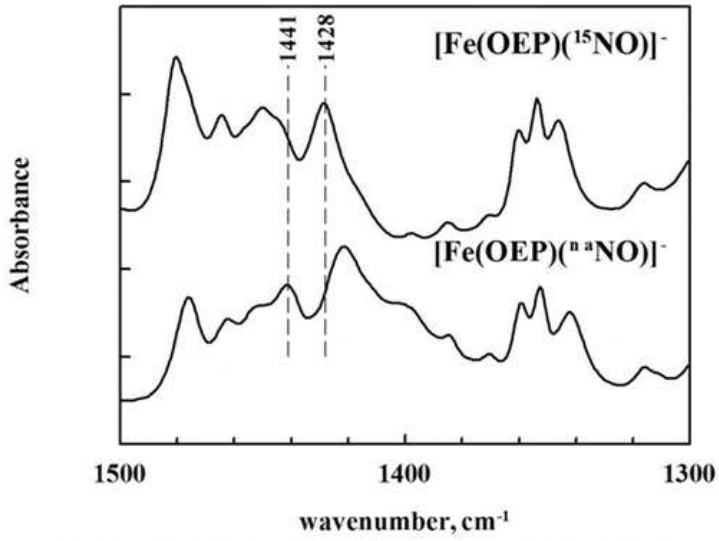

Figure 3. FTIR spectra of [K(2.2.2)][Fe(OEP)(^{na}NO)] and [K(2.2.2)][Fe(OEP)(^{15}NO)] in KBr pellets, where na = natural abundance. Frequencies shown are for ν_{NO} (1441 cm^{-1} for natural abundance, 1428 cm^{-1} for ^{15}N isotopomer).

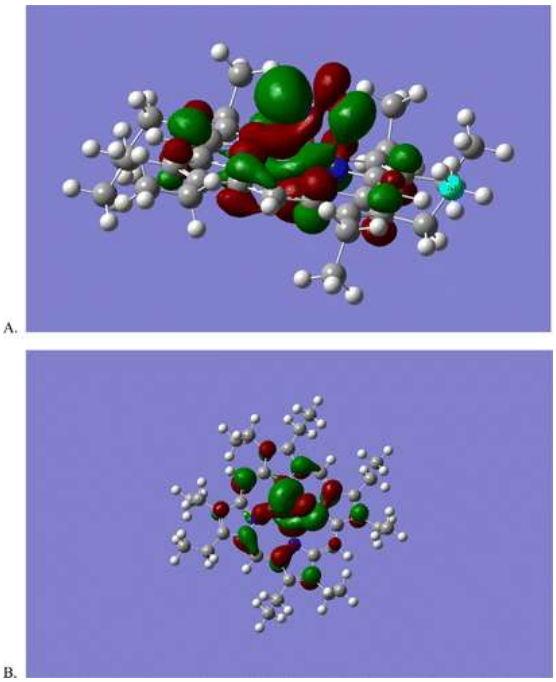

Figure 4. Two views of the HOMO orbital for $[Fe(OEP)(NO)]^{-}$ as calculated using DFT and the m06L functional: (A) side view; (B) top view.

Within the porphyrin ring, the C_β–C_β bonds shortened slightly from 1.365/1.360 Å in the two Fe(OEP)(NO) structures to 1.357 Å in **2**. Given the differences in the two structures of **1**, this decrease is probably not significant and is consistent with little to no electron

density at these positions in the HOMO (Figure 4B). The average C_{meso} bonds were essentially unchanged upon reduction (1.383/1.379 Å in **1** to 1.381 Å in **2**). On the other hand, while the distances from the C_{meso} to the two adjacent C_{α} atoms differed little in **1** (maximum difference 0.005 Å), there was significantly more asymmetry in **2**. While one set of bonds was reasonably symmetrical (1.381/1.379 Å), the other three were much more asymmetrical, going from 1.389/1.378 Å to 1.392/1.374 Å. While this asymmetry was not observed in the DFT calculations, the HOMO orbital in Figure 4B shows bonding interactions between some of the C_{meso} atoms and C_{α} of one pyrrole, but no electron density between the same C_{meso} and the other pyrrole C_{α}. Therefore, the bonding interaction, leading to the asymmetry, is predicted by DFT but is experimentally stronger than that predicted. Therefore, as was seen with the C_{meso}–C_{α} distances, the changes predicted by DFT are in the right direction but are underestimated. Additionally, DFT calculations predicted no significant changes in the planarity of the porphyrin ring upon reduction (DFT: average deviation of 0.036 Å in **1** versus 0.038 Å in **2**).

In calculating the infrared spectra by DFT, it was found from previous studies on related complexes[25] that a scale factor of 0.94 was appropriate for the m06 functional and 1.0 for the bp86 and mpwvwn functionals, though the bp86 functional tended to underestimate the vibrational energies. The results are shown in Table 2. All of the DFT calculations predict a large decrease in the ν_{NO} band upon reduction (1480–1530 cm^{-1}), though none of them predicted correctly the measured wavenumber (1441 cm^{-1}). The mpwvwn functional gave the best agreement (1480 cm^{-1}), which is consistent with the work of Ling et al.,[36] who had previously reported excellent agreement with this functional and the experimental values for nitrosyl complexes.

While $[Fe(OEP)(NO)]^{-}$ is a $S = 0$ complex, the NMR spectrum was significantly different from those of other $S = 0$ metalloporphyrin complexes. Typical values of chemical shifts for such porphyrins, e.g., $Mg^{II}(OEP)$ and $Fe^{II}(OEP)(pyridine)_2$, are 10.0 ppm for the meso-protons and 4.0 and 1.9 ppm for the methylene and methyl protons, respectively.[37,38] The proton NMR spectrum for **2** showed no resonances around 10 ppm, in contrast to what has been seen for typical of $S = 0$ metalloporphyrins. Resonances for anthracene were

observed at 7.4, 7.95, and 8.4 ppm (indicated by asterisks in Figure 5). Additional resonances were observed at 7.50, 7.57, and 7.77 ppm, which are attributed to $[Fe(OEP)(NO)]^-$. In order to confirm this, the NMR chemical shifts were calculated using Gaussian 09. Resonances for the meso proton resonances were predicted at 7.0 and 7.7 ppm. For comparison, the NMR spectrum of Zn(OEP) (S = 0) was calculated using Gaussian, and the calculated chemical shift was found to be 10.7 ppm (experimental: 10.1 ppm[39]). The average calculated resonances by Gaussian for the methylene and methyl protons in $Fe(OEP)(NO)^-$ were 3.1 and 1.4 ppm. This compares to the experimental values of 4.1 and 1.9 ppm for the methylene and methyl protons of Mg(OEP) and the calculated values for Zn(OEP) of 4.4 and 2.0 ppm. Resonances were observed for $[Fe(OEP)(NO)]^-$ at 0.9/1.3 ppm (methyl) and 3.3/3.9 ppm (methylene), both upshifted from the S = 0 values, as predicted by DFT. Further confirmation was obtained by the synthesis of $[Fe(OEP\text{-}d_4)NO]^-$, where the meso protons were replaced by deuterium atoms. Figure 5 shows a comparison between the natural-abundance and d_4 forms of $[Fe(OEP)(NO)]^-$. In the d_4 complex, the resonances attributed to the meso protons were missing or highly attenuated. This spectrum is unusual in comparison to those for other S = 0 complexes. To test whether the chemical shift and splitting for the meso protons were due to the displacement of the iron atom, the DFT calculations for $[Fe(OEP)(NO)]^-$, where the Fe atom was moved into the plane defined by the four pyrrole nitrogens (while maintaining the Fe–N–O bond lengths and angle), were performed. This calculation showed that the average δ value decreased from 7.6 to 9.2, closer to the experimental value for S = 0 metalloporphyrins, but the splitting of the meso protons was more pronounced. Both DFT calculations (Fe out of plane and in plane) showed that the meso protons that were displaced toward the NO group had δ values lower than those displaced away from the NO group. Attempts to mimic this with a five-coordinate S = 0 complex (zinc octaethylporphyrin) in the presence of an excess of 1-methylimidazole-d_3 were inconclusive. The complex did show a small decrease in the chemical shift of the meso resonances (10.18 to 9.99) but no splitting of the meso protons. This shift may have been attenuated because of the facile exchange of the imidazole ligand and the fact that the complex was weak. The most likely source of the splitting of the meso protons may be due to slow rotation of the NO^- ligand around the iron. Slow rotation of the NO^- moiety would

Inorganic Chemistry, Vol 55, No. 5 (2016): pg. 2070-2075. DOI.

more closely mimic the DFT calculations. Further studies are in progress on this issue.

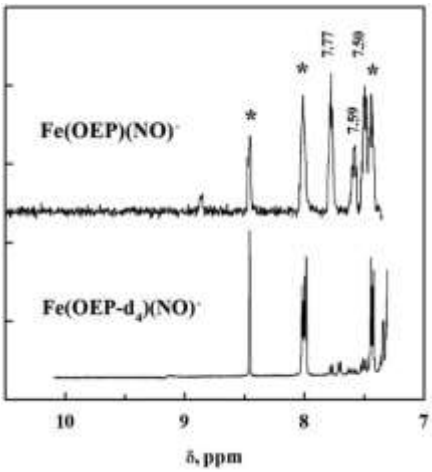

Figure 5. ^{1}H NMR spectra for $[Fe(OEP)(NO)]^{-}$ (natural abundance and d_4 isotopomer). Peaks with asterisks indicate resonances for anthracene. Chemical shifts (δ) for resonances of meso protons are shown.

Conclusions

The changes in the planarity from **1** to **2** were an unexpected result of the reduction. DFT calculations had predicted minor changes. The most significant changes in bond distances were the C_{meso} to C_{α} distances, where the differences in the two C_{meso}–C_{α} distances are probably the sources of the saddling of the complex. While such asymmetry was not predicted by the DFT calculations, the presence of bonding interactions in the HOMO between the C_{meso} and one of the C_{α} atoms is probably the source of this difference. This saddling is not necessarily a consequence of low-valent iron porphyrins, as $Fe(TPP)^{-}$ has an average deviation of less than ±0.05 Å.[40] The metal–N–O angle in the complex was quite similar to those of other $\{M–N–O\}^{8}$ complexes such as **3** and Co(OEP)(NO).[28] Little change was observed in the displacement of the iron atom from the plane in the formation of **2**, unlike the changes observed in the formation of **3**.[21] In both **2** and **3**, the average Fe–N_p bond distances decreased by a similar amount. The decrease in the ν_{NO} band upon reduction was consistent with the increase in the N–O bond length, but the DFT calculations consistently underestimated the wavenumber decrease. Finally, the iron porphyrin nitroxyl showed a unique ^{1}H NMR spectrum for **2**, but the spectrum was consistent with DFT calculations. Overall, the results of this work confirm that the primary site of the reduction of low-spin heme {Fe-

NO}^{7} complexes is on the nitrosyl moiety, as has been observed elsewhere.[14] This result is in strong contrast to the non-heme {FeNO}^{7}, where the reduction is centered on the iron in forming the {FeNO}^{8} complex.[41] This difference is also reflected in the redox potentials, which is much more negative for the heme {Fe-NO}^{7} complexes.

The authors declare no competing financial interest.

References

[1] Fukuto, J. M.; Dutton, A. S.; Houk, K. N. ChemBioChem 2005, 6, 612– 619, DOI: 10.1002/cbic.200400271

[2] Paolocci, N.; Katori, T.; Champion, H. C.; St. John, M. E.; Miranda, K. M.; Fukuto, J. M.; Wink, D. A.; Kass, D. A. Proc. Natl. Acad. Sci. U. S. A. 2003, 100, 5537– 5542, DOI: 10.1073/pnas.0937302100

[3] Irvine, J. C.; Ritchie, R. H.; Favaloro, J. L.; Andrews, K. L.; Widdop, R. E.; Kemp-Harper, B. K. Trends Pharmacol. Sci. 2008, 29, 601– 608, DOI: 10.1016/j.tips.2008.08.005

[4] Hino, T.; Matsumoto, Y.; Nagano, S.; Sugimoto, H.; Fukumori, Y.; Murata, T.; Iwata, S.; Shiro, Y. Science 2010, 330, 1666– 1670, DOI: 10.1126/science.1195591

[5] Nakahara, K.; Tanimoto, T.; Hatano, K.; Usuda, K.; Shoun, H. J. Biol. Chem. 1993, 268, 8350– 8355

[6] Daiber, A.; Shoun, H.; Ullrich, V. J. Inorg. Biochem. 2005, 99, 185– 193, DOI: 10.1016/j.jinorgbio.2004.09.018

[7] Speelman, A. L.; Lehnert, N. Acc. Chem. Res. 2014, 47, 1106– 1116, DOI: 10.1021/ar400256u

[8] Olson, L. W.; Schaeper, D.; Lançon, D.; Kadish, K. M. J. Am. Chem. Soc. 1982, 104, 2042– 2044, DOI: 10.1021/ja00371a051

[9] Lançon, D.; Kadish, K. M. J. Am. Chem. Soc. 1983, 105, 5610– 5617, DOI: 10.1021/ja00355a014

[10] Choi, I.-K.; Ryan, M. D. Inorg. Chim. Acta 1988, 153, 25– 30, DOI: 10.1016/S0020-1693(00)83352-6

[11] Mu, X. H.; Kadish, K. M. Inorg. Chem. 1988, 27, 4720– 4725, DOI: 10.1021/ic00299a009

[12] Choi, I.-K.; Liu, Y.; Feng, D.; Paeng, K. J.; Ryan, M. D. Inorg. Chem. 1991, 30, 1832– 1839, DOI: 10.1021/ic00008a028

[13] Wei, Z.; Ryan, M. D. Inorg. Chem. 2010, 49, 6948– 6954, DOI: 10.1021/ic100614h

[14] Goodrich, L. E.; Roy, S.; Alp, E. E.; Zhao, J.; Hu, M. Y.; Lehnert, N. Inorg. Chem. 2013, 52, 7766– 7780, DOI: 10.1021/ic400977h

[15] Scheidt, W. R.; Frisse, M. E. J. Am. Chem. Soc. 1975, 97, 17– 21, DOI: 10.1021/ja00834a005
[16] Scheidt, W. R.; Duval, H. F.; Neal, T. J.; Ellison, M. K. J. Am. Chem. Soc. 2000, 122, 4651– 4659, DOI: 10.1021/ja993995y
[17] Bohle, D. S.; Hung, C. H. J. Am. Chem. Soc. 1995, 117, 9584– 9585, DOI: 10.1021/ja00142a035
[18] Nasri, H.; Haller, K. J.; Wang, Y.; Huynh, B. H.; Scheidt, W. R. Inorg. Chem. 1992, 31, 3459– 3467, DOI: 10.1021/ic00042a023
[19] Scheidt, W. R.; Lee, Y. J.; Hatano, K. J. Am. Chem. Soc. 1984, 106, 3191– 3198, DOI: 10.1021/ja00323a022
[20] Pellegrino, J.; Bari, S. E.; Bikiel, D. E.; Doctorovich, F. J. Am. Chem. Soc. 2010, 132, 989– 995, DOI: 10.1021/ja905062w
[21] Hu, B.; Li, J. Angew. Chem., Int. Ed. 2015, 54, 10579– 10582, DOI: 10.1002/anie.201505166
[22] Liu, Y. M.; DeSilva, C.; Ryan, M. D. Inorg. Chim. Acta 1997, 258, 247– 255, DOI: 10.1016/S0020-1693(96)05547-8
[23] Bonnett, R.; Gale, I. A. D.; Stephenson, G. F. J. Chem. Soc. C 1967, 1168– 1172, DOI: 10.1039/j39670001168
[24] Frisch, M. J.; Trucks, G. W.; Schlegel, H. B.; Scuseria, G. E.; Robb, M. A.; Cheeseman, J. R.; Scalmani, G.; Barone, B.; Mennucci, B.; Petersson, G. A.; Natatsuji, H.; Caricota, M.; Li, X.; Hratchian, H. P.; Izmaylov, A. F.; Bloino, J.; Zheng, G.; Sonnenberg, J. L.; Hada, M.; Ehara, M.; Toyota, K.; Fukuda, R.; Hasegawa, J.; Ishida, M.; Nakajima, T.; Honda, Y.; Kitao, O.; Nakai, H.; Vreven, T.; Montgomery, J. A., Jr.; Peralta, J. E.; Ogliaro, F.; Bearpark, M.; Heyd, J. J.; Brothers, E.; Kudin, K. N.; Staroverov, V. N.; Kobayashi, R.; Normand, J.; Raghavachari, K.; Rendell, A.; Burant, J. C.; Iyengar, S. S.; Tomasi, J.; Cossi, M.; Rega, N.; Millam, N. J.; Klene, M.; Knox, J. E.; Cross, J. B.; Bakken, V.; Adamo, C.; Jaramillo, J.; Gomperts, R.; Stratmann, R. E.; Yazyev, O.; Austin, A. J.; Cammi, R.; Pomelli, C.; Ochterski, J. W.; Martin, R. L.; Morokuma, K.; Zakrzewski, V. G.; Voth, G. A.; Salvador, P.; Dannenberg, J. J.; Dapprich, S.; Daniels, A. D.; Ö. Farkas; Foresman, J. B.; Ortiz, J. V.; Cioslowski, J.; Fox, D. J. Gaussian 09, Revision D.01; Gaussian, Inc., Wallingford, CT, 2009.
[25] Tutunea, F.; Atifi, A.; Ryan, M. D. J. Electroanal. Chem. 2015, 744, 17– 24, DOI: 10.1016/j.jelechem.2015.02.024
[26] Tutunea, F.; Ryan, M. D. J. Electroanal. Chem. 2012, 670, 16– 22, DOI: 10.1016/j.jelechem.2012.01.027
[27] Wachters, A. J. H. J. Chem. Phys. 1970, 52, 1033– 1036, DOI: 10.1063/1.1673095
[28] Fujita, E.; Fajer, J. J. Am. Chem. Soc. 1983, 105, 6743– 6745, DOI: 10.1021/ja00360a049

[29] Ellison, M. K.; Scheidt, W. R. Inorg. Chem. 1998, 37, 382– 383, DOI: 10.1021/ic971109j
[30] Kelly, S.; Lançon, D.; Kadish, K. M. Inorg. Chem. 1984, 23, 1451– 1458, DOI: 10.1021/ic00178a030
[31] Godbout, N.; Sanders, L. K.; Salzmann, R.; Havlin, R. H.; Wojdelski, M.; Oldfield, E. J. Am. Chem. Soc. 1999, 121, 3829– 3844, DOI: 10.1021/ja9832820
[32] Busing, W. R.; Levy, H. A. Acta Crystallogr. 1964, 17, 142– 146, DOI: 10.1107/S0365110X64000408
[33] Li, J.; Noll, B. C.; Schulz, C. E.; Scheidt, W. R. Angew. Chem., Int. Ed. 2009, 48, 5010– 5013, DOI: 10.1002/anie.200901434
[34] Belhaj Ali, B.; Belkhiria, M. S.; Daran, J. C.; Nasri, H. Acta Crystallogr., Sect. E: Struct. Rep. Online 2012, 68, m1262– m1263, DOI: 10.1107/S1600536812038317
[35] Davlieva, M. G.; Lü, J. M.; Lindeman, S. V.; Kochi, J. K. J. Am. Chem. Soc. 2004, 126, 4557– 4565, DOI: 10.1021/ja049856k
[36] Yang, L.; Ling, Y.; Zhang, Y. J. Am. Chem. Soc. 2011, 133, 13814– 13817, DOI: 10.1021/ja204072j
[37] Dolphin, D.; Sams, J. R.; Tsin, T. B.; Wong, K. L. J. Am. Chem. Soc. 1976, 98, 6970– 6975, DOI: 10.1021/ja00438a037
[38] Buchler, J. W.; Eikelmann, G.; Puppe, L.; Rohbock, K.; Schneehage, H. H.; Weck, D. Ann. Chem. 1971, 745, 135– 151, DOI: 10.1002/jlac.19717450117
[39] Fuhrhop, J. H. Z. Naturforsch., B: J. Chem. Sci. 1970, 25, 255– 265, DOI: 10.1515/znb-1970-0305
[40] Mashiko, T.; Reed, C. A.; Haller, K. J.; Scheidt, W. R. Inorg. Chem. 1984, 23, 3192– 3196, DOI: 10.1021/ic00188a032
[41] Speelman, A. L.; Lehnert, N. Angew. Chem., Int. Ed. 2013, 52, 12283– 12287, DOI: 10.1002/anie.201305291